

**Accepted January 9<sup>th</sup>, 2025.****URETERAL PERISTALTIC FLOWS IN THE PRESENCE OF MICROLITHS: A REVIEW****P. Deepalakshmi<sup>1</sup>, D. Tripathi<sup>2</sup>, G. Shankar<sup>3</sup>, O. Anwar Bég<sup>4</sup>, S. Kuharat<sup>5</sup> and E. P. Siva<sup>6\*</sup>**<sup>1,3,6\*</sup> *Department of Mathematics, College of Engineering and Technology,**SRM Institute of Science and Technology, Kattankulathur – 603203, Tamil Nadu, India*[dp5497@srmist.edu.in](mailto:dp5497@srmist.edu.in); [sg1710@srmist.edu.in](mailto:sg1710@srmist.edu.in); [sivae@srmist.edu.in](mailto:sivae@srmist.edu.in)<sup>2</sup>*Department of Mathematics, National Institute of Technology, Uttarakhand-246174, India.*<sup>4,5</sup>*Multi-Physical Engineering Sciences Group, Dept. Mechanical and Aeronautical Engineering,**Corrosion/Coatings Lab, 3-08, SEE Building, Salford University, Manchester, M54WT, UK.*[dtripathi@nituk.ac.in](mailto:dtripathi@nituk.ac.in); [O.A.Beg@salford.ac.uk](mailto:O.A.Beg@salford.ac.uk); [S.Kuharat2@salford.ac.uk](mailto:S.Kuharat2@salford.ac.uk),\*Corresponding author E-mail: [sivae@srmist.edu.in](mailto:sivae@srmist.edu.in)**Abstract**

A detailed review is presented on research contributions in peristaltic transport in the human ureter in the presence of microliths. The studies reviewed are differentiated based on methodologies deployed, namely analytical, numerical and CFD simulation techniques and also experimental (clinical) investigations. Various 2-D and 3-D models are discussed along with more advanced Fluid Structure Interaction (FSI) studies. The propagation of the incompressible urine flow results in reflux nephropathy. As such, the peristaltic waves spread near the outlet of the tube which manifests in a depletion in the flow rate. Due to the maximum pressure gradient, urine backflow occurs. A full understanding of ureter reflux has however not yet been achieved. This review surveys approximately 101 journals addressing the obstruction inside the ureter and the associated hydrodynamics. As such it consolidates many different efforts in the field in a single source which will serve as a guide to both clinical researchers (e. g. physicians) and also mathematical and engineering research groups and is hoped that it will assist in the development of new integrated approaches for robust treatments. The extensive survey of the scientific literature in this review article confirms that stones (monoliths) detected in the proximal part of the nephron are generally larger than those identified in distal parts. These papers defined the position and shapes of microliths. Due to bolus transport inside the ureter flow, varying pressure and velocity balances are also appraised. The more advanced FSI simulations provide much-

needed insight into visualizing actual ureteral transport. Some future pathways for collaborative efforts in improving healthcare for patients are also suggested.

**Keywords:** *Computational Fluid Dynamics, Fluid Structure Interaction, Ureter hydrodynamics, Peristalsis; Trapping Bolus, Visualization.*

## 1. Introduction

### 1.1 General Characteristics

The average length of the human ureter is between 7 to 10cm.<sup>[1]</sup> Within that short tract numerous functions are performed by the kidney. The actual transport of blood through the kidney has been investigated extensively.<sup>[2,3]</sup> Also, an executive model <sup>[4]</sup> was presented on renal physiology. The ultimate function of ureter is *micturition* (or urination which is the emptying of urine from the urinary bladder).<sup>[5,6]</sup> The bladder is the human urinary storage system and comprises detrusor smooth or involuntary muscle. The urethral muscles consist of the external and internal sphincter. The kidney first undergoes glomerular filtration for separating minerals and unwanted particles from blood. This is followed by tubular absorption and finally secretion of essential elements to neutralize the blood.<sup>[7]</sup> The anatomical structure of the human urinary systems is depicted in **Fig. 1**.

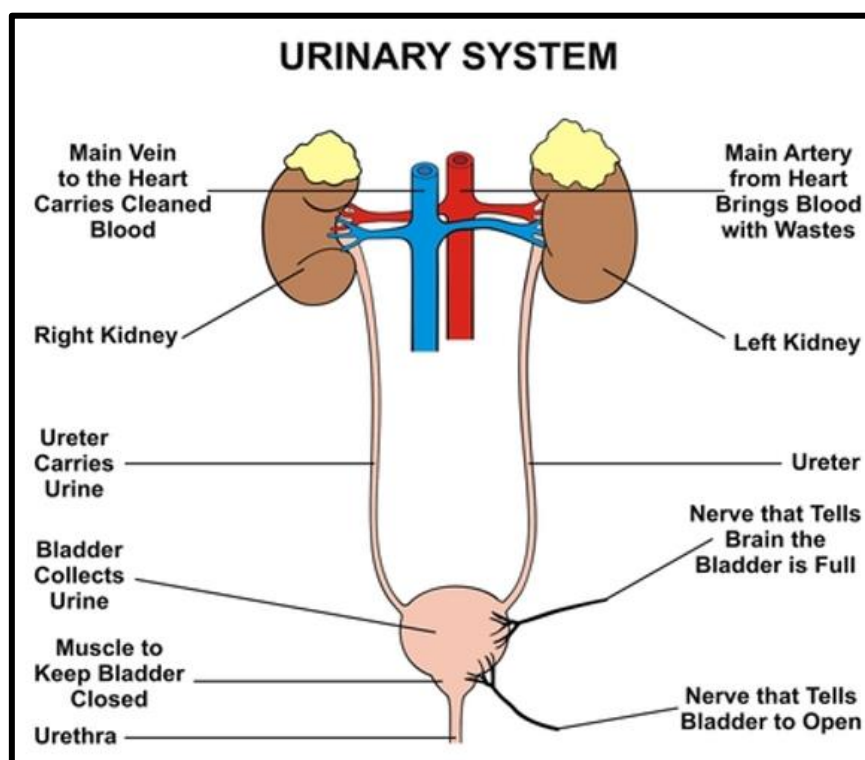


**Fig. 1:** The human urinary system [from wikipedia.org]

As soon as the urine is discharged to the renal pelvis from the calyces, the contraction process starts.<sup>[8]</sup> This initiates the generation of sinusoidal wave form termed peristaltic motion. Both contraction and expansion take place in peristaltic waves.<sup>[9]</sup> During this stage, certain minerals are deposited and remain along the wall of ureter. The major systematic peristaltic process begins at the *proximal stage* in the pelvic region filled with smooth cells known as ‘atypical’ muscle cells.<sup>[10]</sup> Transport in the proximal tubule is characterized with 3-D ureter flow.<sup>[11]</sup> Subsequently, the depositions are transformed into *microliths* (small stone deposits) which can cause severe pain during urination in humans. To circumvent or mitigate these situations, a number of diverse procedures are used in medicine.<sup>[12]</sup> Both experimental and theoretical/computational studies of ureteral impedance due to monoliths have been conducted in both human subjects and also other mammals. Generally, three pathways for calculi formation have been identified in detail which are observed commonly in the pelvic region of human ureter.<sup>[13]</sup> The key aspects of ureteral transport with video recordings based on clinical surveys of 50 urinary systems.<sup>[14]</sup> Important experiments have been done on rodent subjects to clarify the transport defects in renal tubules.<sup>[15]</sup> Here, the focus was the size of microliths formation inside the ureter. Important analytical studies of ureteral dynamics have generalized the simpler Newtonian flow model to consider more sophisticated rheological models. Other studies have also considered heat transfer. The exploration of viscoelastic ureteral flow in a slanted cylindrical geometry with the Jeffrey model.<sup>[16]</sup> Other non-Newtonian models employed in recent years include Eringen’s micropolar model which was deployed for using the low Reynolds number and long wavelength approximations of lubrication theory and also considering heat transfer.<sup>[17]</sup> Another key aspect of ureteral transport studies has been fluid structure interaction (FSI). The ureter is a muscular tube with non-linear mechanical properties which conveys urine, as noted earlier, from the kidneys to the bladder via peristalsis. This process is essentially a biological fluid-structure interaction mechanism which requires deformable conduits. In the urinary system, the peristaltic motion is induced by a muscular contraction of the ureteral wall initiated by pacemakers which pumps the urine from the kidney to the bladder through the ureter. Ureteral peristaltic motions are therefore characterized by a complicated movement of a range of aligned muscle fibres in the ureteral wall. The walls of the ureter deform via the fluid transport which in turn deform the fluid- this two-way dynamic interaction is extremely sophisticated and generally requires the use of computational mechanics software e. g. ANSYS, ADINA, COMSOL, OPENFOAM etc. Very few studies of 3-D FSI of peristalsis have been communicated in the literature, whether related to blood flow

or urine transport. The ANSYS CFD code was utilized to compute Newtonian and non-Newtonian peristaltic pumping with the Carreau and power-law models, also for visualizing the vorticity and trapping bolus patterns carefully.<sup>[18]</sup> Computational fluid dynamic (CFD) software has great potential in simulating in 3-D the characteristics of for example Extrinsic Ureteral Obstruction (EUO). Later in this review, relevant studies will be appraised in this regard. The article will also provide a very useful single source of benefit to both industrial and biomedical sectors which may assist in mobilizing a concerted effort to mitigate ailments associated with the disturbance of urinal flow patterns. An extensive range of topics is included herein and both analytical and computational studies are examined. Articles addressing the hydromechanical efficiency of the pelvic region are highlighted. Two major factors of relevance to peristaltic pumping are reflux and trapping phenomena which constitute intensive areas of modern research in both applied mathematics and biomechanical engineering. The vast majority of studies reviewed in this article have been found to focus on the basic mechanism of peristaltic propulsion inside the ureter, the associated variations in pressure caused and the geometric deformations in urinary tract vessels (tubes, channels etc). It is envisaged also that the current article will be of use to both mathematical and clinical researchers (physicians) in the continued efforts to relieve patients from suffering with calculi formation.

## **2. Analytical Studies**

Early mathematical focused on peristaltic motion in the human oesophagus. These did not correlate closely with biological data collections. Later, more comprehensive hydrodynamic models were developed, and analytical and numerical solutions were shown to qualitatively agree with experimental data.<sup>[19]</sup> Earlier models were based on viscous-dominated flows and utilized the lubrication theory, neglecting inertial effects. Later asymptotic expansions were used to consider higher order viscous and inertial effects in peristaltic pumping in a tube by including the nonlinear advection terms in the equations of motion.<sup>[20]</sup> That demonstrates that the reflux (mean flux in the negative axial direction in a layer of fluid adjacent to the wall when the net mean flux is positive) arises whenever an adverse mean pressure gradient is present, and this is independent of the peristaltic wave form. Significantly later, considerable progress has been made in simulating steady ureteral dynamics with a collapsible tube model approaching the physics with a “compressive zone” model, valid at both low and high Reynolds numbers.<sup>[21]</sup> The confirmation done using lubrication theory that peristaltic pumping of urine from the kidney into the bladder occurs at comparatively small mean flow rates, during which

isolated boluses of urine are displaced gradually via the ureter by the contraction waves. It also determined that an upper limit to the mean flow rate exists with steady peristaltic propulsion, which is strongly influenced by the mechanical properties of the ureter. At excessively high flow rates the peristaltic contractions obstruct the transport of urine through the ureter and pumping is highly inefficient. A coupled fluid-structure interaction model has been deployed for ureteral pumping, combining wall deformation and unsteady fluid flow, thin-shell and lubrication theories, with smooth muscle activation based on clinical data.<sup>[22]</sup> They focused on the activation wave of muscular contraction and conducted for the case of an infinite tube, theoretical (small amplitude) and numerical computations. They considered several important physiological features including phase-lag in wall constriction, lumen occlusion (associated with thickening lumen material with contracting smooth muscle) and simulated the bolus dynamics. They identified several contributory factors which damp the hydromechanical efficiency of pumping, namely elastic and hydrodynamic properties of the ureter associated with ailments and further showed that while a linear flow rate-pressure rise relationship is present for weak to moderate activation waves, it becomes nonlinear when the lumen contracts to a closed position. It has also been established that during ureteral peristaltic pumping, the muscular activity creates a contraction wave that propels the bolus of urine along the ureter and the pressure rises to a peak and then diminishes to a threshold level, as depicted in **Fig. 2**.

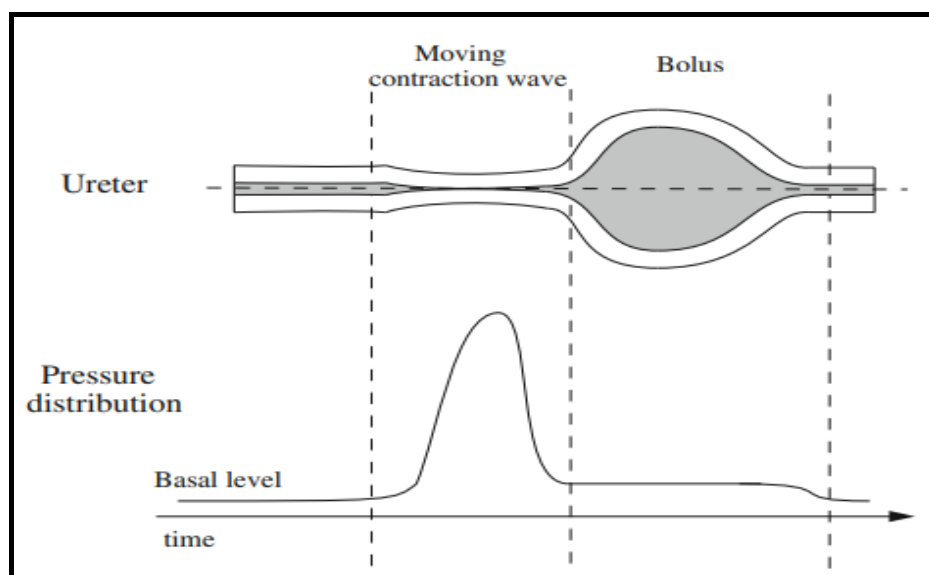


**Fig. 2.** Pressure distribution during bolus transport in the human ureter <sup>[2]</sup>

During urine flow, certain mineral-based deposits (e. g. monoliths) may be formed due to few chemical depositions in ureter.

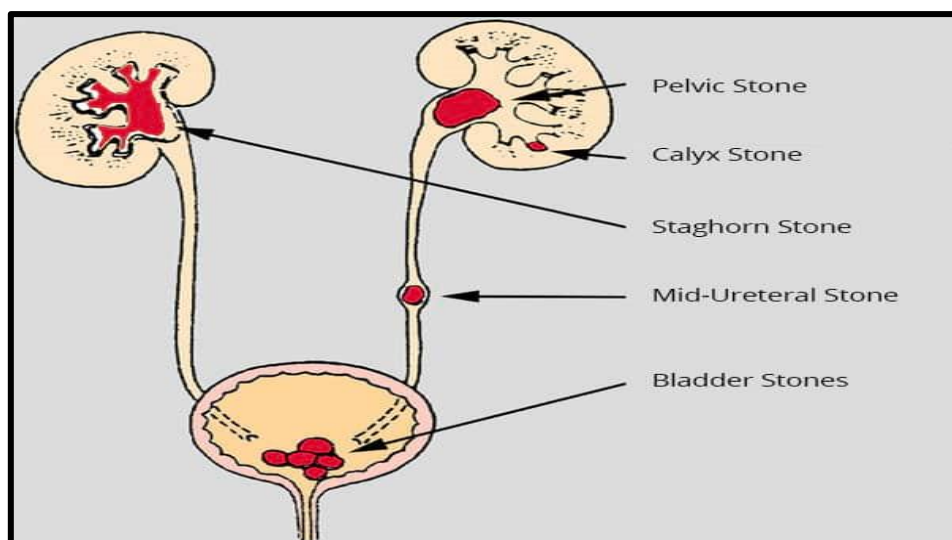


**Fig. 3:** The human urinary system- courtesy Dr. Tim Nathan, Urology, Sunshine Coast University Private Hospital, Queensland, Australia

These masses may originate in the kidney and move into the ureter. A stone begins when particles of minerals in stagnated urine crystallize and form a mass. The stone-like structural depositions induce extremely severe pain to humans during urination. If the ureter is occupied by either stones or bacterial infections, this can lead to long-lasting pain. **Fig. 3** depicts the many types of these stones which can arise in the human urinary system. **Fig. 4** further elaborates the multiple processes involved in producing human urine, an extremely complex sequence of events.

### **2.1 Newtonian ureteral hydrodynamic studies**

Perturbation solutions were derived for time-dependent Newtonian peristaltic pumping in a two-dimensional channel model of the ureter containing a geometric obstruction (stone).<sup>[23]</sup> They examined the creeping dynamics for the stone modelled as a small rigid sphere including Stokes drag, virtual mass, Faxén, Basset and gravity force effects. They computed flow streamlines, velocity profiles and pumping rates achieving good agreement with experiments. They also visualized particle trajectories for scenarios involving stone deposits comprising calcium oxalates for calculosis and *Escherichia coli* type for bacteria and noted that retrograde or reflux motion of the particles and also bacterial conveyance may arise in the upper urinary tract when there is a *partial occlusion of the peristaltic wave*. Theoretical study has been done on the particle dispersion in a two-dimensional ureteral peristaltic flow with zero pressure rise, observing that forward or reflux motion of the wave is strongly dependent on the degree of

occlusion of the peristalsis.<sup>[24]</sup> They also noted that the particle trapping efficiency is elevated with wave amplitude ratio.

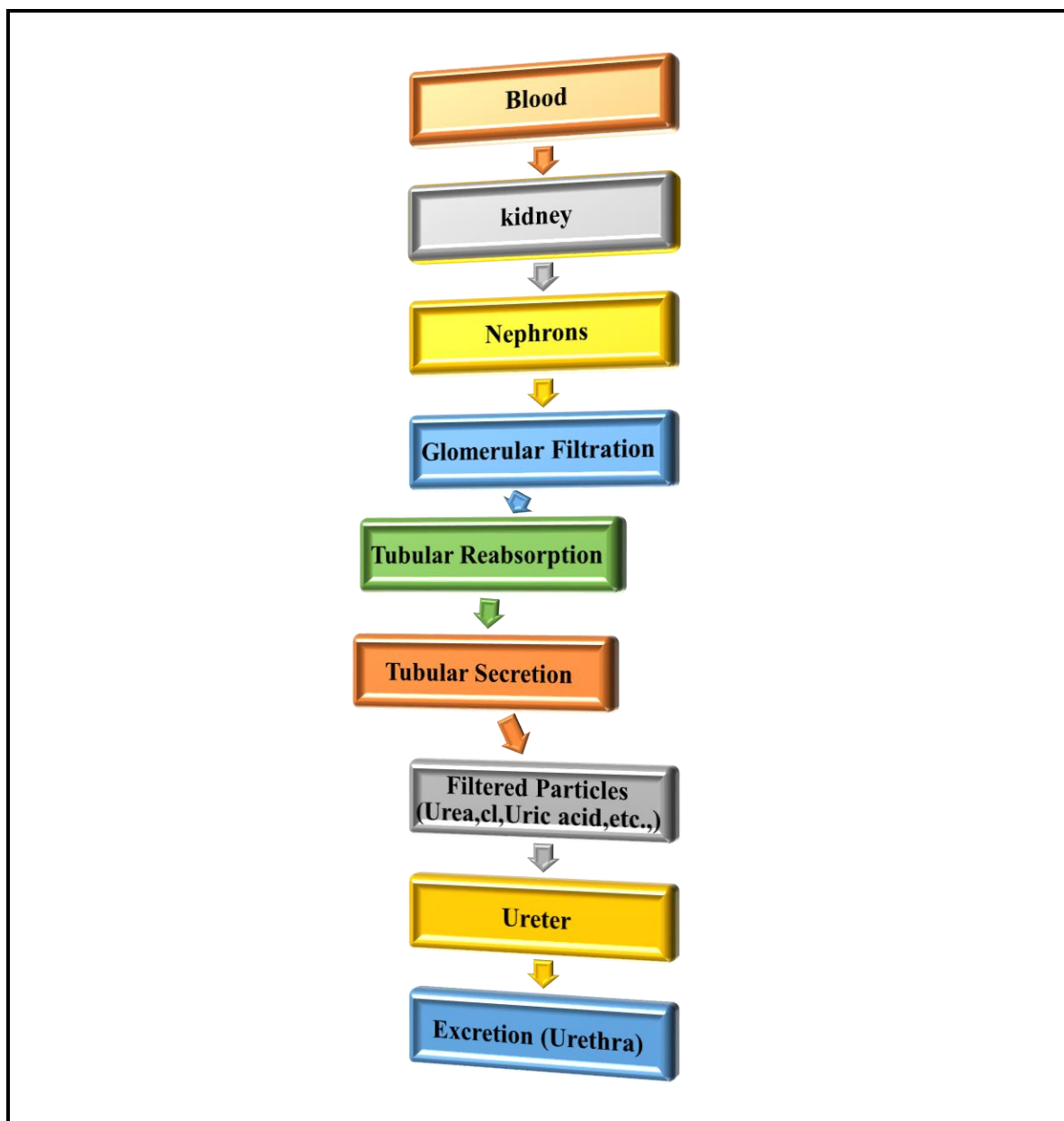


**Fig. 4** Detailed mechanism of urine formation

## 2.2 Non-Newtonian Ureteral hydrodynamic studies

An extensive number of theoretical and numerical studies of ureteral peristalsis have been reported in the literature. Numerical methods are required for resolving nonlinearity associated with rheological characteristics. Many different techniques have been applied in recent years and are summarized in **Fig. 5**. Some popular non-Newtonian models are given in **Fig. 6**. The immersed boundary method (IBM) is just one example of an extremely versatile and accurate numerical scheme used in peristaltic hydrodynamics and other biological propulsion

simulations. The popularity of numerical methods is largely due to the facility of coding complex material models through in-house programs, since the commercial computational fluid dynamics (CFD) software do not offer the full range of material models. A notable study in this regard in which the IBM has been successfully applied with an Oldroyd-B rheological formulation to compute the complex characteristics of ureteral obstruction (single solid particle) peristaltic dynamics with two-way coupling between the viscoelastic fluid and the particle.<sup>[25]</sup>



**Fig. 5:** Numerical methods deployed in ureteral peristaltic simulations.

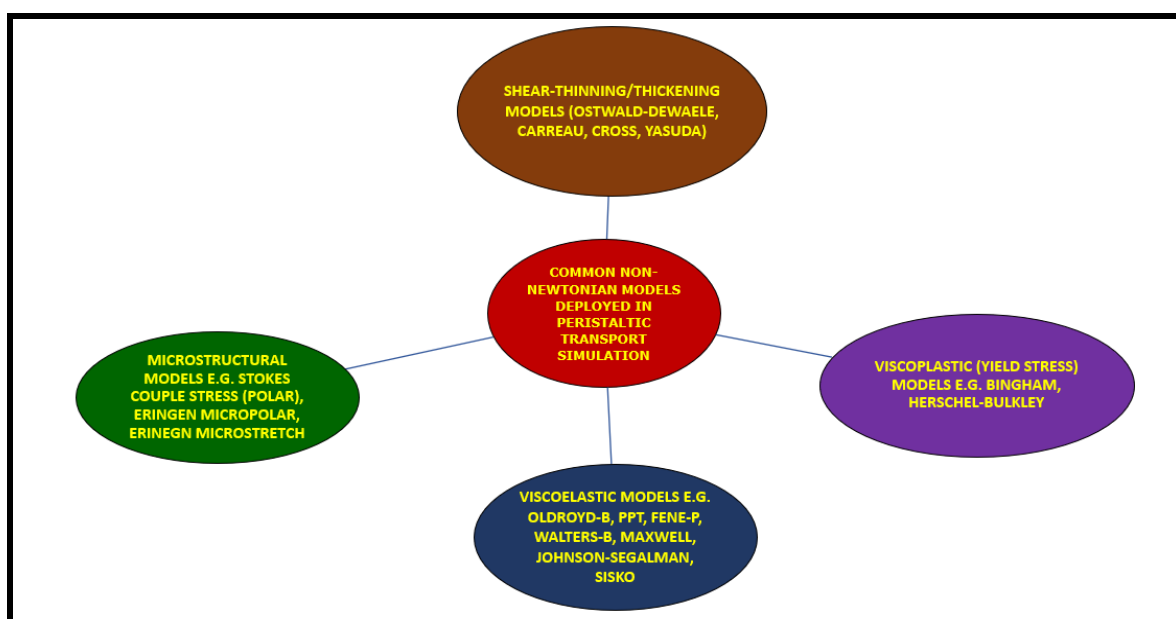


**Fig. 6:** Popular non-Newtonian models used in ureteral hydrodynamics.

They employed a square computational domain with side length equal to one wavelength of the channel and periodic boundary conditions at the walls. Eulerian discretization was employed with a uniformly spaced MAC (marker and cell) grid. Second-order accurate Kim-Moin projection, Adams-Bashforth and Crank-Nicholson techniques were utilized for the temporal discretization of viscous and convective terms. In the IBM formulation, Eulerian force density was specified as a Dirac delta function layer of force supported by the immersed boundaries, and a regularized delta function with compact support was utilized to spread the Lagrangian elastic forces from the immersed boundaries. Stiffness constants were implemented to enforce the traveling waves along the ureteral channel domain. They obtained excellent agreement for the Newtonian creeping flow case (vanishing Weissenberg number and unity Reynolds number) in the absence of a solid particle.<sup>[26]</sup> Generalized IBM simulations were conducted for Reynolds number of unity, Weissenberg number (ratio of elastic to viscous force) of 5, a particle (monolith) of radius  $r = 0.075$  initially placed along the centerline of a channel with occlusion ratio = 0.4 and aspect ratio = 1.5. **Fig. 7** shows the contour visualizations deployed to determine the impact of the solid particle on stress fields for times  $t = 1, 4$  and  $12$ , for either no particle (top row) and in a channel with the particle (bottom row). Their results confirm that peak stress distension is located in the contracted region of the ureteral channel both with and without the monolith, although evidently higher values arise for the latter case. A key observation of this study was that reflux is induced only when the monolith is located in the most constricted zone and is therefore pumped backwards. The stress build-up in the contraction accelerates the reverse motion.

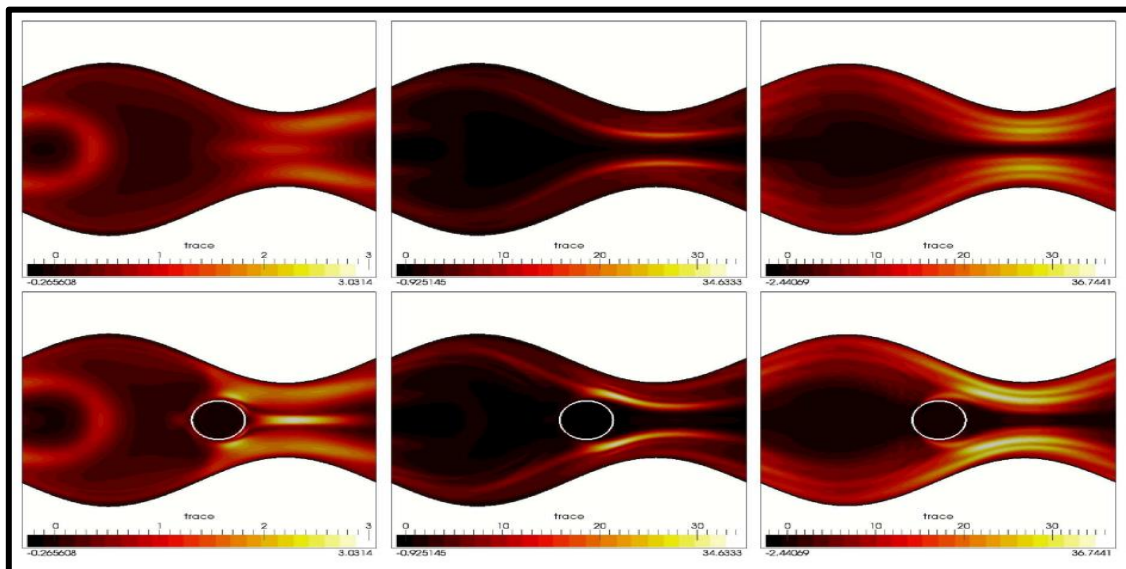


**Figure 7:** Stress contour plots at  $t = 1, t = 4,$  and  $t = 12$  without (top) and with a solid particle (below).<sup>[25]</sup>

Other non-Newtonian investigations include variable viscosity formulation to compute the rheological effects in peristaltic transport in a non-uniform tube and channel considering two-layered fluid model (peripheral and core flow zones).<sup>[28]</sup> Since curvature is also intrinsic to the ureteral system, other investigators have explored two-dimensional peristaltic rheological pumping in curved geometries.

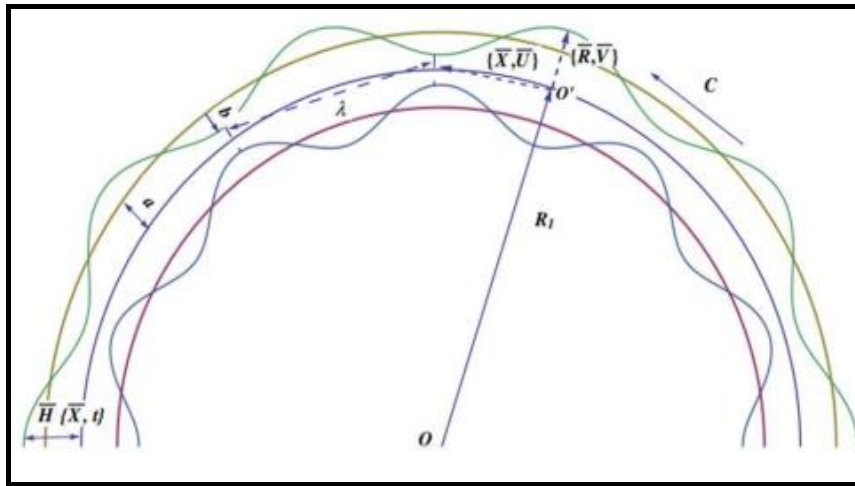


**Figure 8:** Curved ureteral peristaltic model of Riaz and Sadiq<sup>[29]</sup> [Reproduced with permission]

The Saffman-Marble fluid-particle suspension (dusty) model was utilized in conjunction with the Eyring-Powell rheological model to study analytically the transport of solid particles in non-Newtonian laminar incompressible urine dynamics in a diseased, symmetric, curved distensible-walled channel geometry representing the ureter (**Fig. 8**).<sup>[29]</sup> Perturbation solutions were derived and showed that increasing concentration of solid particles depletes both velocity and pressure magnitudes and significantly modifies the pumping characteristics of the liquid. They further showed that increasing curvature of the channel also inhibits peristaltic transport and manifests in a clustering of particles at the lower zone of the channel. They further computed the influence of various parameters on the circulating bolus trapping (**Fig. 9**) and observed that the number of boluses increased with greater curvature, whereas for the particulate phase streamlines, the number of boluses is reduced to one with higher curvature. However, this study did not explicitly address the rheological effects associated with the Eyring-Powell model. Further studies include the Stokes couple stress fluid model and Saffman particle suspension model to compute the peristaltic pumping in a ureteral geometry under magnetic field, as a simulation of magnet-assisted therapy.<sup>[30]</sup> They used Mathematica software

to evaluate the pressure and velocity distributions and showed that stronger magnetic field inhibits pumping in the core zone whereas increasing concentration of solid particles suppresses flow along the entire duct. They further noted that pumping rate is depressed with higher couple stress (non-Newtonian) parameter and bolus size and quantity are reduced with greater magnetic field.

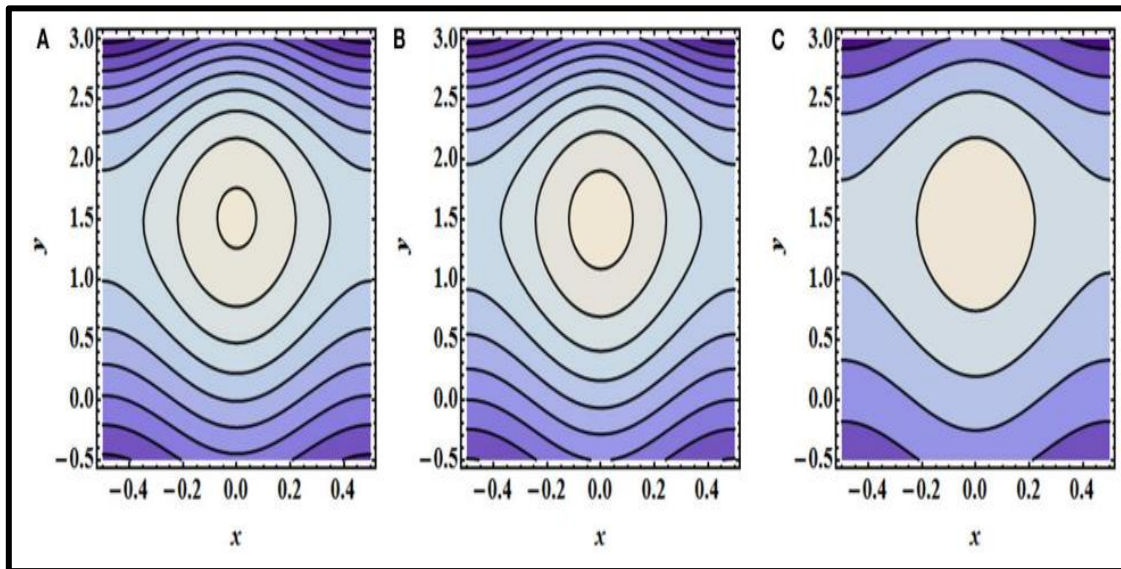


**Figure 9:** Trapping bolus visualization for fluid phase with concentration parameter = 3 and different values of curvature parameter (A) 3.1, (B) 3.2 and (C) 3.3.<sup>[29]</sup>

### 3. CFD/FSI Simulations

The inherent geometric complexity of the urinary system means that analytical and numerical (2-D) simulations, as described in the previous sections are gross approximations. The actual system is 3-dimensional, and the biological tissue is very complex. Many of these challenges have been summarized lucidly including detrusor hyperactivity, renal function interplay, nonlinearity of the ureteral biomaterial, complex interactions of compression waves, adhesion of stones to the ureteral wall and so on.<sup>[31,32]</sup> The accurate analysis of realistic ureteral peristaltic transport therefore necessitates 3-D computer modelling and engineers have dominated this area for decades, rather than mathematicians. The basic methodology of finite element analysis (FEA) underpins the commercial software platforms available for 3-D simulations which may be purely fluid (CFD) or combined fluid-structure interaction models (FSI). These so-called field solvers include ADINA-FSI, ANSYS, ABAQUS, COMSOL, OPENFOAM, MARC, NASTRAN, PHOENICS, SOLIDWORKS and many others. In certain cases, due to axi-symmetry of the geometry, 2-D simulations can be utilized which still retain

much of the essential physics. Here we shall review several of the most interesting contributions in computational simulations reported in recent years. A detailed study utilizing the ADINA-FSI software (developed by MIT's K.J. Bathe, founder of ADINA R & D, 1986) has been presented.<sup>[33]</sup>

They assumed linear elastic, isotropic properties of the ureter wall with a Young's modulus of 0.5 MPa. The urine is assumed to be Newtonian with density of  $\rho = 1050 \text{ kg/m}^3$  and viscosity of  $\mu = 1.3 \text{ c Poise}$ . The constraint function method was deployed to accommodate non-linear contact conditions and 2-D nine-node axisymmetric solid elements for the structure and 2-D three-node axisymmetric fluid elements for the urine flow were used. They also implemented an (ALE) Arbitrary Lagrangian-Eulerian. The fluid wall shear stress behind the contracted wall and the maximum values of shear stress around the throat of the moving contracted wall is suppressed as the peristaltic wave progresses towards the bladder. Close to the entry zone of the ureter in the vicinity of the kidney a much greater shear stress is generated. Numerous other investigations have also been conducted identifying many other aspects of ureteral dynamics including pressure difference ranging from 1 to 0.01mmHg.<sup>[34-37]</sup> Exploration of three different ureter models (**Fig. 10**) and studied the different flow patterns of urine and flow rate through the numerical computation.<sup>[38]</sup> They identified that the luminal rate of flow is principally influenced by the posture of the ureter since this greatly influences peristaltic wave efficiencies.

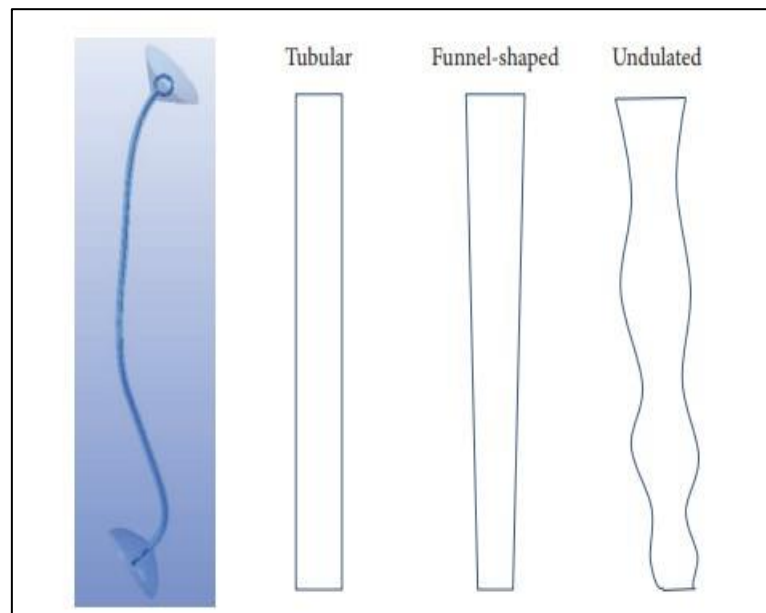


**Fig.10** Three different curved, funnel shaped and undulated models of ureter.<sup>[38]</sup>

CFD FSI simulation showed that the occurrence of inertial forces inside the urine flow which exhibits peristaltic motion, encourage the ureteropelvic junction to resist the reflux particularly

during the commencement of the wave propagation.<sup>[39]</sup> The urine velocity enhances at the bolus location inside the ureter. However, the velocity is suppressed at the neighbouring zone of the bolus when compared to the motion inside the bolus. These computational results have proved quite beneficial in urinary treatments. A further excellent computational study using a different numerical code, COMSOL, has been communicated.<sup>[40]</sup>

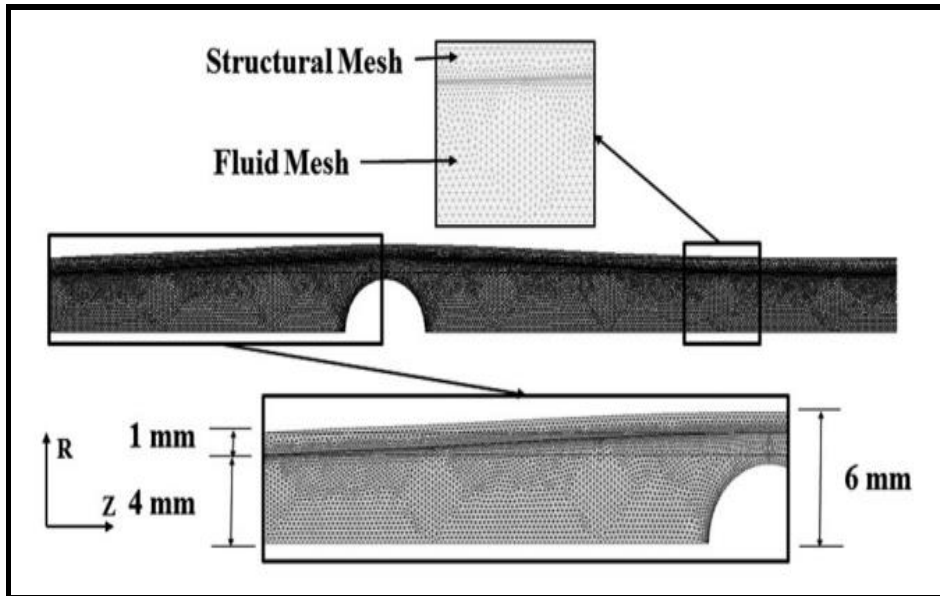


**Fig.11** Geometry and mesh of the fluid and structural domain.<sup>[40]</sup>

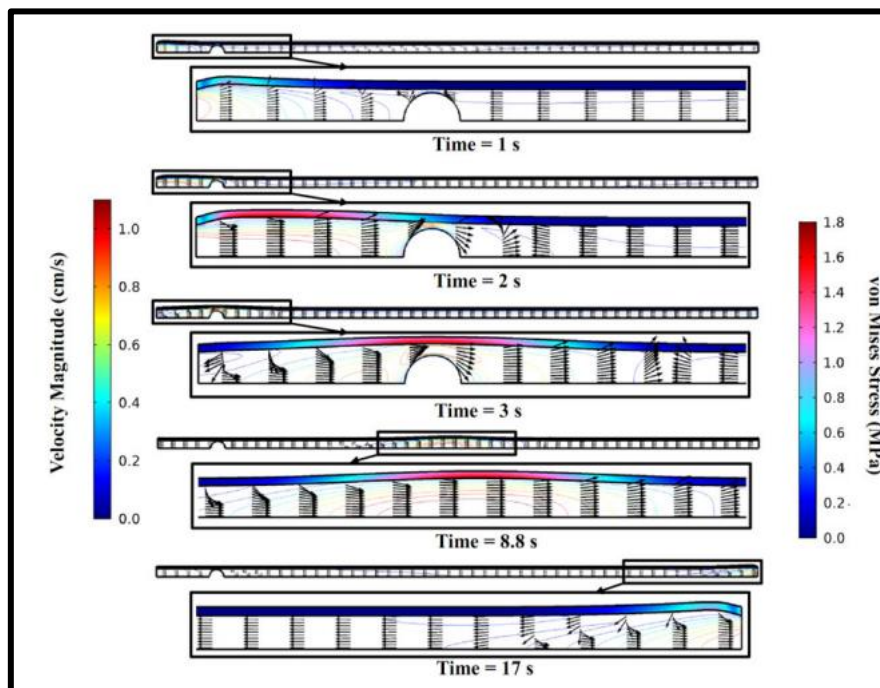


**Fig. 12:** Contours of von Mises stress for the ureter, along with streamlines overlapped with velocity vectors for the fluid flow.<sup>[40]</sup>

Distinct from the study, which assumed a *compressive force*, which struggles to generate a bolus of urine when compressed, deploys *expansive force* on the ureter wall.<sup>[33,40]</sup> They deployed the Boyarsky-Labay data which estimates that urine is transported due to an isolated bolus of sized 3 to 12 cm in length and 1 to 4 mm in width. They constrained both ends of the ureter and considered the case of a stone as a fixed obstruction modelled as a semicircle of 3.6 mm of radius with its centre located 3 cm away from the inlet and resulting in an 81% blockage in the undeformed flow path. The mesh utilized is shown in **Fig. 11**. The fluid structure interaction (FSI) results included both hydrodynamic contours and stress plots, the latter are shown in **Fig. 12**. A key novelty of this work is that it is among the first computational models to include realistic material properties for the human ureter i. e. *anisotropic hyperelastic* behaviour, as opposed to the much more simplistic linear elastic properties assumed in other studies. The FSI model deployed therefore employed at least a layer of meshing between the solid obstruction and the solid ureter wall, and more accurately simulates the solid-solid contact between the stone and the ureteral wall, would be infeasible to model. However, to model a translating obstruction within the ureter is extremely complicated dynamic meshing approach which is also very extensive computationally and requires large compilation times. This study correctly predicted that high peaks in the values of wall shear stress and pressure gradient arise near the stone obstruction (**Figure 13**) and have minimal impact on von Mises stress magnitudes, indicating that a rupture due the presence of obstruction is a very weak possibility.

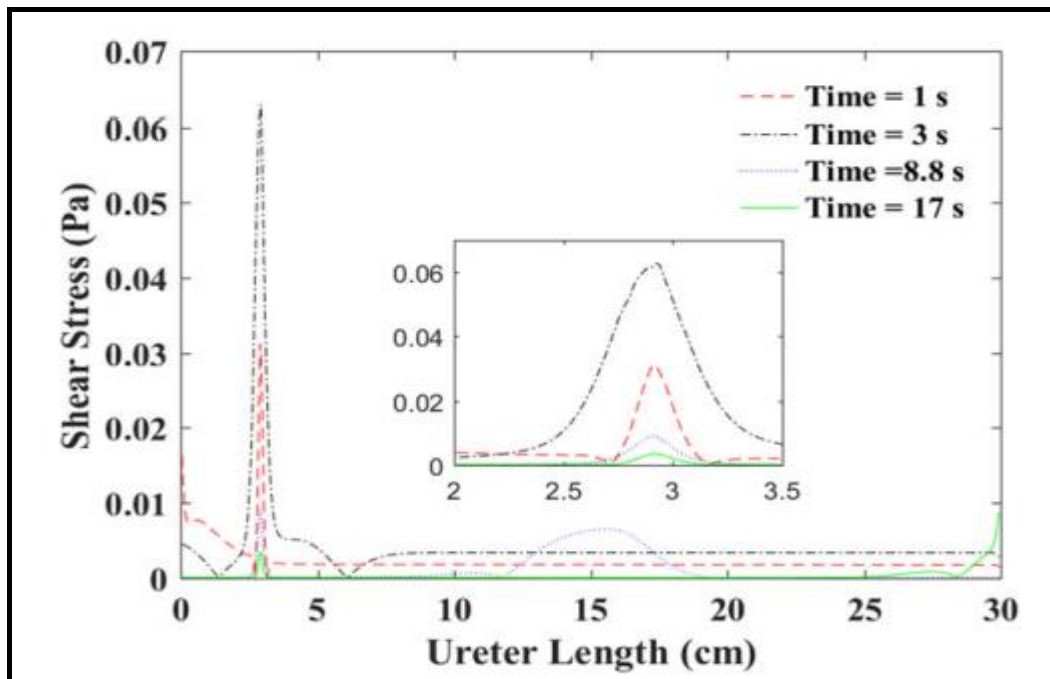


**Fig. 13:** Wall shear stress distribution along the 2-D geometrical model of the ureter wall.<sup>[40]</sup>

ANSYS workbench FSI deployed to simulate 3-dimensional obstructed ureteral peristaltic pumping.<sup>[41]</sup> They utilized spherical stone obstructions and varied the size as 5% (2mm), 15% (3 mm) and 35% (4 to 6 mm) are taken into consideration. **Fig. 14** visualizes the velocity distributions for all three stones. They also assessed the influence of stone shape comparing the effects of sphere to those of cubical and star-shaped stones, all at a fixed obstruction percentage of 15%. They noted that a larger obstruction manifests in stronger flow reversal, higher pressure gradients and amplified wall shear stresses in the vicinity of the obstruction. Star-shaped stones were also observed to produce maximum pressure gradient whereas cube-shaped stones generated the strongest flow reversal. A key deduction of this study was that stone shape does not markedly modify the wall shear stress for the obstruction percentage considered.

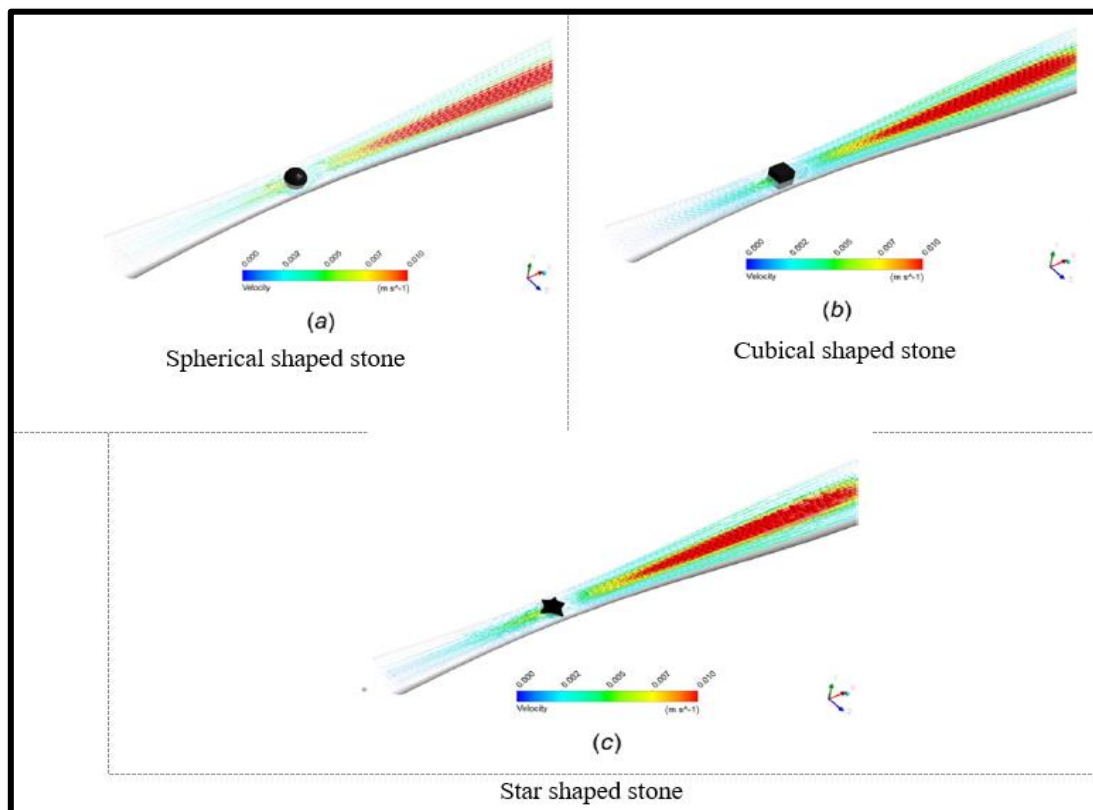


**Fig. 14** (a-c) velocity distribution for three different types of stone formation inside ureter.<sup>[41]</sup>

ABAQUS commercial software deployed to simulate numerically the fluid-structure interaction between urinal fluid and a double-J stented ureter.<sup>[42]</sup> They implemented three material models for an isotropic ureteral wall, namely the Mooney-Rivlin, Yeoh and Ogden

constitutive formulations. They modelled the length of a healthy ureter from the Ureteropelvic Junction (UPJ) to the Vesicoureteral Junction (VUJ) i. e. a 28 cm distance.

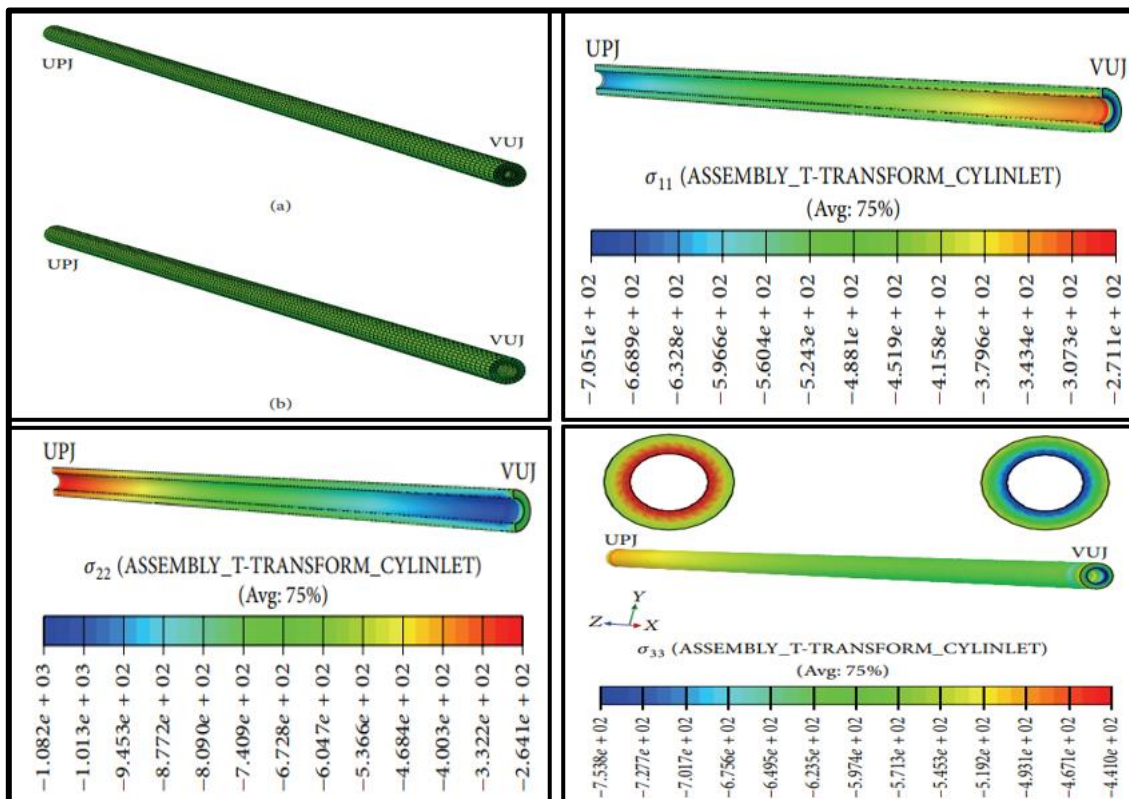


**Fig. 15:** Top left - Fluid domain mesh (a) and solid domain mesh (b). Top right- Radial stresses distribution. Below left- Circumferential stresses distribution. Below right- Tangential stress distribution.<sup>[42]</sup>

The stented ureter (opened after the muscle tone vanishes) was simulated as a cylindrical tube with both length and wall thickness of 1 mm and an internal 3mm diameter. The fluid domain was discretized with 16800 hexahedral linear elements (FC3D8 elements in the ABAQUS Elements Library) and the structural (solid) domain meshing for the ureter utilized 10080 hexahedral linear continuum elements (C3D8H). The stent was analysed as a cylinder coaxially disposed with the ureter and with 1mm diameter. Their FEA simulations are shown in **Fig. 15**. They showed that the Ogden model achieves the most accurate representation due to its ability to reproduce the lower zone region of the stress-strain curve behaviour and that all stresses (radial, circumferential and tangential) generated by urine peristaltic pumping in addition to the intra-abdominal pressures have relatively low magnitudes. This indicated that in the studied pressure regime, the ureter exhibits rigid body (non-deformable) characteristics. ABAQUS finite element software was utilized in addition to a detailed mechanical formulation for *stone/ureter interaction*, to compute the initial separation angle and radial stress distribution between the spherical obstruction geometry and ureteral tube wall.<sup>[43]</sup> They

also benchmarked their computations with *in vitro* experimental measurements. The kidney stone was treated as a rigid sphere with radius variation and a static friction coefficient of 0.5 was utilized, based on SEM images of uric acid stone for the average friction coefficient between kidney stone and ureter. A Fung-type constitutive elastic model was deployed for the ureter. 4-node bilinear axisymmetric quadrilateral, hybrid elements (CAX4RH) were utilized.

**Fig. 16** shows the finite element ABAQUS model with different radius ratios.

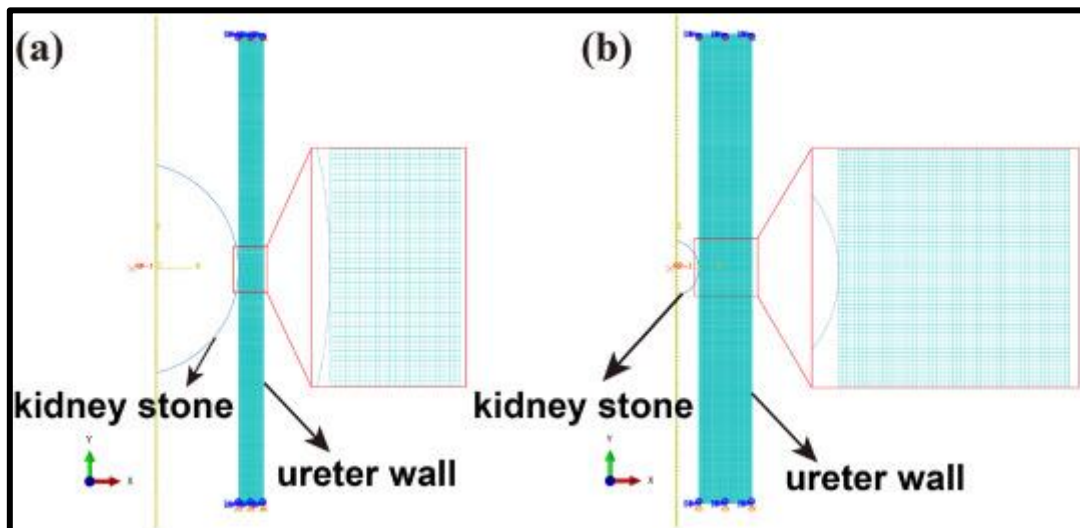


**Fig. 16:** Stress distribution and deformation in ureter caused by a kidney stone: (a) FE model of kidney stone and ureter with radius ratio = 1.3, and (b) FE model of kidney stone and ureter with radius ratio = 3.4<sup>[43]</sup>

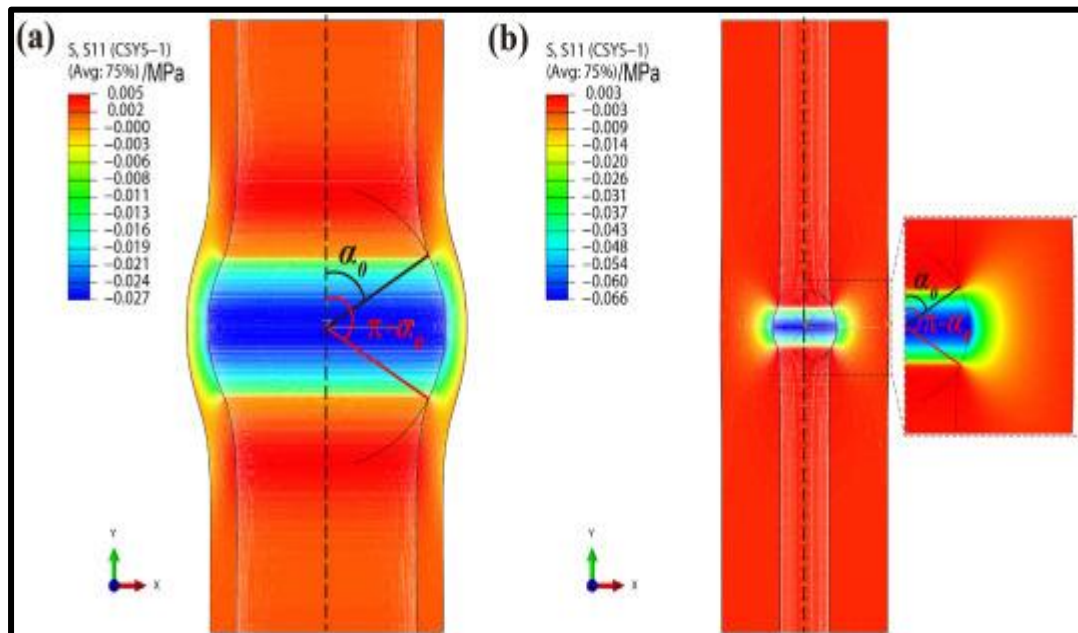


**Fig. 17** (a) Compression stress distribution and deformation in ureter due to spherical kidney stone with radius ratio of 1.3. (b) Compression stress distribution and deformation of ureter caused by kidney stone with  $\eta = 3.4$  <sup>[43]</sup>

**Fig. 17** depicts the stress and deformation contour plots. This study identified that the critical diameter of kidney stones is 11%–22% larger than the inner diameter of ureter; however, there is a negative correlation of kidney stone magnitude to the confining pressure outside the ureter which inhibits ureteral pumping efficiency.

#### 4. Combined Numerical and Experimental Studies

In addition to purely analytical, numerical and commercial CFD FSI simulations, other researchers have also explored *both experimental and numerical modelling* of ureteral peristalsis with and without obstructions. Ureteral experiments studies conducted on three female dogs for picturing the pressure distribution in renal pelvis.<sup>[44]</sup> They showed that obstructions inside the ureter brings undefined pain during urination and depositions adhere inside the ureter and the flow depends upon the magnitude of deposition. 2-dimensional ANSYS finite volume simulations of peristaltic contractions in obstructed ureter flows were reported.<sup>[45]</sup> They used the Patankar SIMPLE algorithm with clinical experimental data to investigate the influence of different percentage obstructions (0%, 5%, 15% & 35%) for spherical stones with a major focus the maximal stone size of 35% obstruction.<sup>[46]</sup> They showed that backflow is 20 times larger in obstructed cases when compared to the unobstructed ureter. **Fig. 18** visualizes their pressure distributions during contraction and expansion stages of the peristaltic motions.

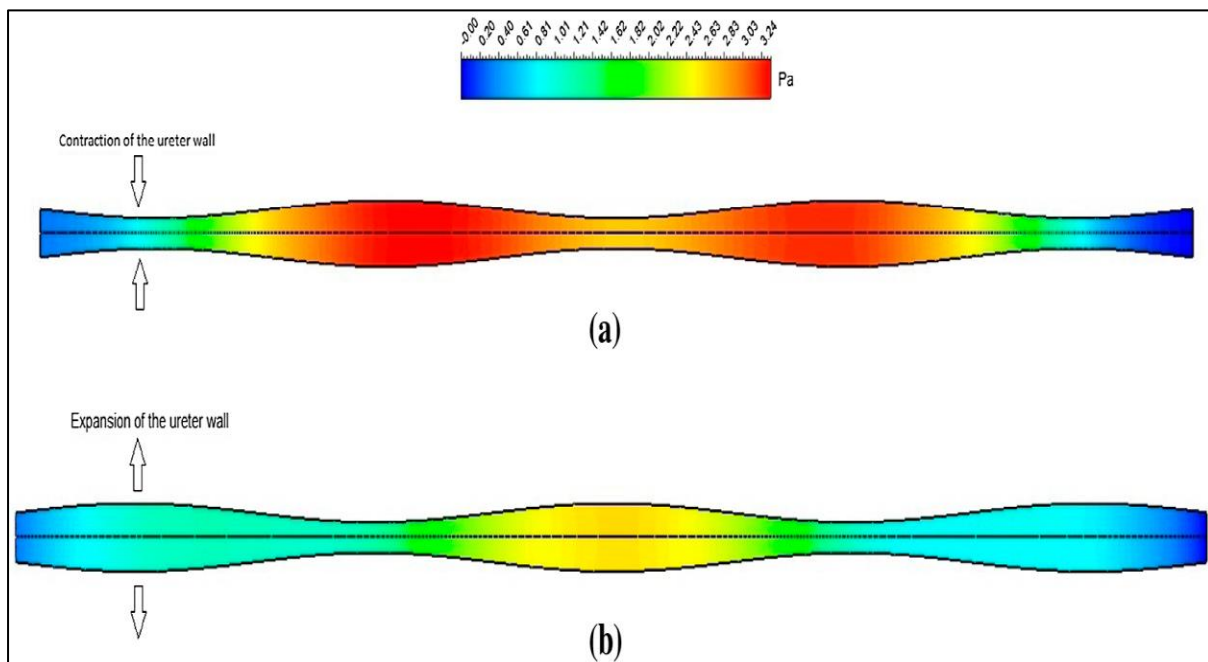


**Fig.18** Ureter pressure contours at two intervals of contraction and expansion a)  $T/4$  and b)

$3T/4$  <sup>[45]</sup>

2-D and 3-D FSI ANSYS simulations were performed on the obstruction in ureteral pumping.<sup>[47]</sup> They concentrated on stones with 5mm diameter which can enter the ureter walls. They showed that stones larger than 5mm, do not have ability to enter into the ureter. These large diameter stones will stay in the pelvis itself and they settle therein. The authors visualized cases with radii of 50% (2.8mm) and 70% (3.4mm). They studied the elevation in the obstruction size with rise in the amount of back flow. The wall shear stress and pressure gradient values were observed to peak at the obstruction. They noted a slight deviation in wall shear stress values in obstructed cases compared to the unobstructed cases. They also identified a high amount of backflow in obstructed ureter and the contrary behaviour in the unobstructed ureter. They further emphasized that obstruction in the interior part of the ureter can precipitate several severe diseases including urinary tract infections. Peristaltic flow characteristics in diseased ureteral situations experimentally examined, considering the effects of pharmacodynamics, intraluminal pressure, flux and other characteristics.<sup>[48]</sup> Non-intrusive examining voiding dysfunction in ureteral obstructions encountered in older patients, focusing on urine transport characteristics in the prostatic urethra (PU) with bladder outlet obstruction (BOO).<sup>[49]</sup> They generated detailed normal PU and three phase models with 3D-CAD software tracing cystourethroscopic images. They prescribed a normal detrusor pressure to the bladder side in each model and showed that a sizeable vortex arises close to the bladder outlet (BO) with increased hydraulic energy loss accompanying transport via the tract. The opening of the BO section however removes this vortex and suppresses hydraulic energy losses. They obtained excellent correlation with clinical measurements based on catheterized pressure sensors inserted into the urethra in addition to urethral diameter urethrographic measurements. Other studies have explored multiple physical effects in ureteral peristalsis. Investigation done on electrical field effects on ureteral peristaltic flow with heat transfer effects.<sup>[50]</sup> Urine transport with a COMSOL finite-element-based solver with a two-way fully coupled fluid structure interaction approach between the ureter wall and urine.<sup>[51]</sup> **Fig. 19** shows the mesh design utilized. They analysed the ureter wall as an anisotropic hyper-elastic material based on experimental data and propulsion was simulated as a series of isolated boluses. They observed that the peristalsis mechanism has a natural tendency to create a backflow as the isolated bolus moves forward. They also analysed the flow of urine through ureter to bladder at the interval of timing includes 1,6.5,12 &17 seconds respectively. As a result, the urine can flow backwards

from the bladder to the ureter at the ureterovesical (ureter-bladder) junctions, if the one-way valve starts to malfunction.

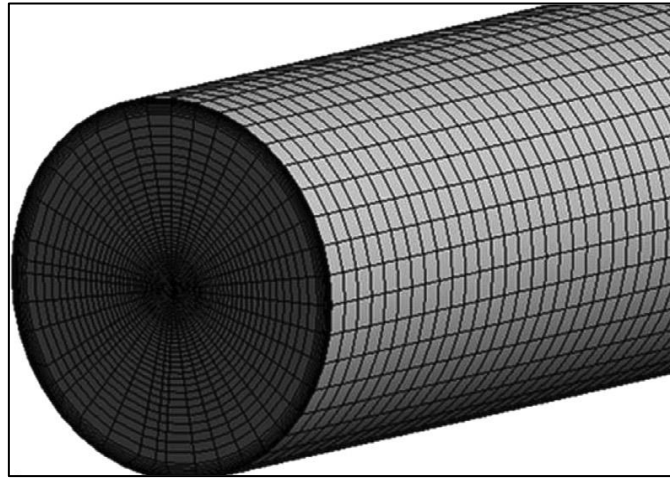


**Fig. 19** Ureter with mesh design.<sup>[53]</sup>

Analysis on ureter flow described that when the ureteral reflux becomes low due to the large amount of pressure difference occurs between kidney and urinary bladder.<sup>[52]</sup> They concentrated on reducing the occurrence of reflux. They studied the characteristics of stented ureter impact on the flow. This stent permits the ureter walls to have flexibility when the fluid flows with heavy pressure hits the boundary. It also relaxes the wall of the ureter. Thus, both solid structure and fluid structure domains were coupled simultaneously. This research recommended the detailed study of geometry, and also the blockage locations inside the annulus. An additional assessment of ureteral computational fluid structure interaction was reported.<sup>[53]</sup> The geometrical model they studied is shown in **Fig. 20**.

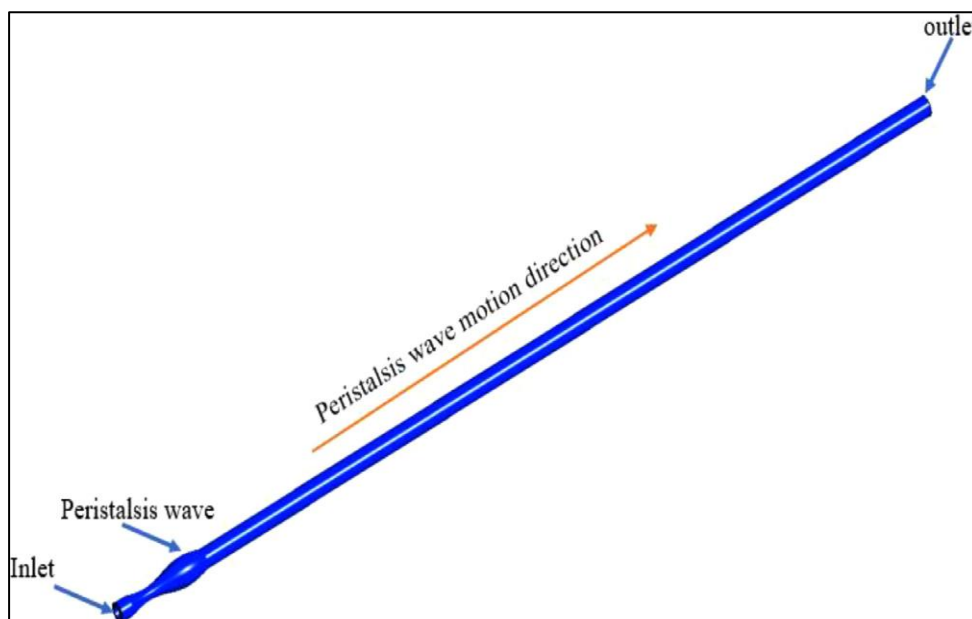


**Fig. 20** Geometry of the Ureter.<sup>[53]</sup>

## 5. Some key findings on ureteral studies

### 5.1. Urinary Obstructions

The magnitude of the trapping bolus was clearly observed.<sup>[54]</sup> Computational works are executed along with real clinical implications. Peristaltic transport simulated in ureteral channel and tube geometrical models.<sup>[55,56]</sup> The equation was unrevealed by expressing stream function by using perturbation solutions.<sup>[57]</sup> Differentiation of the mechanical properties between chronically affected ureters and normal ureters of certain mammals including dogs and humans.<sup>[58]</sup> They also determined clinically that ureteral tissue shows similar properties like other tissues in the body. Research on peristaltic movement in the presence of different obstructions (stones).<sup>[59]</sup> In most of the stones, calcium oxalate content will be very high.<sup>[60,61]</sup> Owing to the prolonged depositions inside the ureter the renal replacement becomes unavoidable in patients.<sup>[62]</sup> These disturbances impact the urinary flow which undergoes changes in flow patterns.<sup>[63]</sup> Several treatments for removing barriers inside the ureter have suggested.<sup>[64]</sup> Discussions on recent developments in the formation of pathogenesis inside the ureter due to chemical depositions like Calcium Oxalate, Calcium Phosphate and Cystine have been explored.<sup>[65]</sup> Urine is generally assumed to be incompressible in mathematical and numerical models. The governing equations for urine are the Navier-stokes equations (mass and momentum conservation) are as follows:<sup>[47]</sup>

$$\nabla \cdot \mathbf{u}_{fluid} = 0 \quad (1)$$

$$\rho \frac{\partial \mathbf{u}_{fluid}}{\partial t} + \rho (\mathbf{u}_{fluid} \cdot \nabla) \mathbf{u}_{fluid} = \nabla \cdot \left[ -p\mathbf{I} + \mu \left( \nabla \mathbf{u}_{fluid} + (\nabla \mathbf{u}_{fluid})^T \right) \right] + \mathbf{F} \quad (2)$$

### 5.2. Bolus Properties over the Wall

Further experimental research summarized proposed that the tissue around the ureter acting as a biologic elastometer.<sup>[66]</sup> They also correlated the physical and mechanical characteristics of ureteral tissue with microscopic validation. Also, there is a gradual enlargement in volume of urine bolus when peristaltic propulsion is intensified.<sup>[67]</sup> Description was given detailly related to ureteral muscle.<sup>[68]</sup> They applied the isometric technique for the evaluation of these muscles. SIMPLE (semi-implicit pressure-linked equation) finite volume approach was used to compute pressure and velocity distributions and to simulate the formation of urine bolus and its effect along the wall of ureter.<sup>[69]</sup> Clinical realistic values were deployed for calculating pressure when the bolus passes through the ureter.<sup>[70]</sup> Pressure differences were observed during reflux which was found to be low when compared to pressure in the bladder.<sup>[71]</sup> The wall shear stress

diminished when the external magnetic field is applied in ureteral magnetic therapy.<sup>[72]</sup> A novel idea was given to record peristaltic contractions using a pacemaker.<sup>[73,74]</sup> New models were implemented for reducing the costs of computational simulation.<sup>[75]</sup> Modelling of a single peristaltic wave assisted in determining the pressure gradient at 4 discrete time intervals with corresponding inlet boundary conditions.<sup>[76]</sup> They employed ANSYS-CFX software. By simulating the pumping actions which diminish the particle concentrations in the flow which is very much helpful for preventing urinary tract Infections.<sup>[77]</sup> These investigations have provided very useful guidance for physicians in utilizing novel treatments effectively. Many of these studies have demonstrated that backflow in the urine is principally attributable to the lower functionality of the ureteropelvic junction relative to the ureterovesical junction.

### ***5.3. Reflux Phenomena***

To address the reflux phenomena in the ureter, a non-linear 2D ureteral model was developed.<sup>[78]</sup> A Mooney-Rivlin model was constructed for bring out the mechanical properties and reflux phenomena happening inside the ureter.<sup>[79,80]</sup> Clinically based numerical study of reflux phenomena inside the ureter has been presented.<sup>[81]</sup> A detailed insight into reflux reaction was presented.<sup>[82,83]</sup> Further studies on reflux response in 2D non-uniform channels were communicated.<sup>[84,85]</sup> Additional studies were conducted on peristaltic ureteral flows inside circular tubes.<sup>[86,87]</sup> Managing Resonance (MR) scans have also been examined and shown that similar reflux reactions occur for children during obstructions.<sup>[88]</sup> In many of these investigations a robust formulation for the ureteral fluid-wall geometry of the tapered channel of urine flow has been utilized which takes the form.<sup>[84]</sup>

$$H_1(X, t^*) = a - X \tan \alpha + b \sin \left( kX - \omega t^* - \frac{\varphi}{2} \right) - \text{lower wall of channel} \quad (3a)$$

$$H_2(X, t^*) = a + X \tan \alpha + b \sin \left( kX - \omega t^* + \frac{\varphi}{2} \right) - \text{upper wall of channel} \quad (3b)$$

### ***5.4. Location of Calculi***

Intraluminal pressure differences were observed in both normal and acute ureter during peristaltic flow.<sup>[89]</sup> The position of calculi and the pressure variations due to the disturbances along the wall was discussed.<sup>[90]</sup> To define the surface of stone, researchers utilized a major technique called CT (Computerized Tomography).<sup>[91]</sup> There are different types of stones deposited inside the ureter. One among those are calcium oxalate stones and its pathogenesis was studied in detail.<sup>[61]</sup> Calculi characteristics were determined by Prstojevic.<sup>[92]</sup> Numerous

tests were conducted among mice to establish changes in ureteral hydrodynamics with and without obstructions.<sup>[93]</sup> The urine flow inside the ureter and also patterns within the stented ureter were simulated using CFD.<sup>[94]</sup> A survey was conducted among 2,38,500 cases to highlight the major problems in ureteral obstruction.<sup>[95]</sup> This study recommended that patients utilize ureteral stents. In certain cases, there may be failure of stents. Hence failure-free stents were tested among 300 patients.<sup>[96]</sup> To reduce failure of stent usage rates, stiff tandem stents were introduced and popularized among patients.<sup>[97]</sup> This Tandem stent is stiff and remains active over long periods.<sup>[98]</sup> The 3-D modelling of stents has been performed using MRI-generated data.<sup>[99]</sup> In these relevant studies, **Table 1** summarizes the major studies reviewed in this article.

**Table 1** Classification based on FSI, Analytical and numerical-focused articles.

Authors Name	Purpose	FSI used	Journal & year of publication	Method	Software used
Vahidi and Fatouraee	Analysed the Reflux reaction inside the ureter	FSI	IEE, 2007 [33]	ALE- (Arbitrary Lagrangian-Eulerian)	ADINA
Vahidi et al.,	Maximum shear stress found across Proximal part of the ureter	FSI	Journal of Biomechanical Engineering, 2011 [37]	ALE	ADINA
Vahidi and Fatouraee	Modelling in ureter will be more useful to physicians to figure out disorders and find better way to cure.	FSI	Journal of Theoretical Biology, 2011 [39]	ALE	ADINA
Takaddus et al.,	Reflux nephropathy happens due to failure of ureteropelvic junction	FSI	International Mechanical Eng. Congress & Exposition 2016 <sup>[40]</sup>	ALE	COSMOL Multiphysics
Najafi et al.,	Stone size will not give substantial effect on ureter wall when the obstruction disturbs the flow.	FSI	Journal of Biomechanical Engineering, 2016 [41]	ALE	ANSYS
Najafi et al.,	Shear stress will reach its peak in case of obstruction when compared to without any obstruction.	FSI	Computer Methods in Biomechanics & Biomedical Engineering, 2017 [45]	ALE	SIMPLE
Takaddus and J Chandy	Variation in Pressure, wall shear stress and reflux nephropathy were observed during obstruction.	FSI	International journal for Numerical Methods in Biomedical Engineering, 2018 [47]	ALE	Finite Element Solver
Takaddus and J Chandy	Observance of peristaltic flow inside the ureter.	FSI	Computer Methods in Biomechanics &	ALE	COSMOL Multiphysics

			Biomedical Engineering, 2018 [51]		
Takaddus et al.,	When the obstruction enhances, reflux nephropathy considered to be increase.	FSI	International Journal for Numerical Methods in Biomedical Engineering, 2018 [57]	ALE	Finite Element Monolithic Solver
Vahidi & Fatouraee	Backflow will be measured along the centre and top surface of the tube due to ureteropelvic junction failure.	FSI	Measurements, 2007 [36]	ALE	ADINA
Haifler et al.,	To reduce Failure of stent usage rate, stiff Tandem stents were introduced.	FSI	Journal of Biomechanics, 2021 [97]	ALE	ADINA
Barzegari et al,	Better comparison was made between clinical and predicted values for ureteric pressure	FSI	Medical & Biological Engineering & Computing, 2020 [101]	ALE	ADINA
Lozano et al.,	The failure of clearing residuals from the upper urinary tract calculi after successful extracorporeal shock wave lithotripsy	Nil	Physical Review E, 2009 [23]	Analytical-perturbation	MATLAB
Riaz and Sadiq	The increase in peristaltic pumping causes a decrease in the solid particle concentration.	Nil	Frontiers in Physics, 2020 [29]	Analytical-perturbation	MATHEMATICA
Keni et al.,	To determine the biomedical characteristic of urinary bladder wall due to change in the volume	Nil	Journal of Mechanics in Medicine and Biology, 2019 [12]	Numerical-FEM	ANSYS
Hosseini et al.,	The high level of wall shear stress and the reflux usually occur at the beginning of the lumen closure.	Nil	Biomedical Engineering Letters, 2017 [81]	Numerical-CFD	CgLes

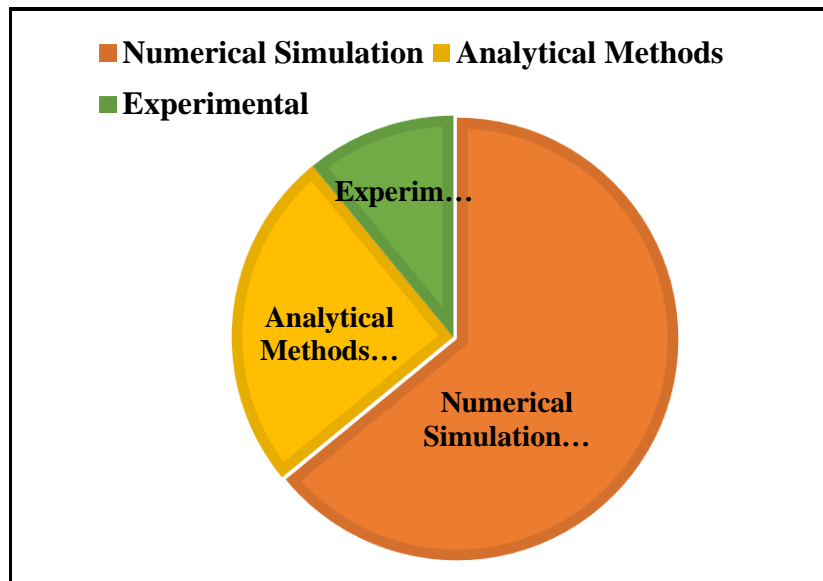


**Fig. 21** Solution procedures executed in articles.

From the analysis, we can conclude that out of 101 journals, 64 papers have examined ureteral peristaltic dynamics with obstructions by a numerical simulation approach, 25 papers have utilized analytical methods and the remaining 12 papers were experimentally based. Hence, by virtue of this review, one has access to an extremely diverse and state-of-the-art collection of key studies using all three scientific approaches- analytical, numerical, and experimental- for ureteral peristaltic transport phenomena.

## 6. Conclusions

An extensive review has been presented of 101 articles addressing theoretical (analytical), computational and experimental studies of ureteral peristalsis with and without obstructions (monoliths). These studies have provided shear stress, velocity, pressure, bolus dynamics and other key characteristics associated with real ureteral dynamics. Back flow has been identified when the pressure of urine reaches negative values at the time of outlet. This has been shown to lead to damage in the Ureterovesical Junction. Many different commercial software has been deployed to analyse fluid-structure interaction (FSI) including ABAQUS, ANSYS/CFX, COMSOL etc. The 2-D and 3-D simulations on FSI have clarified the impact on ureter flow with blockages i.e. solid particles. These investigations have provided excellent visualizations with a range of material models for the ureter wall and different monolith stone (obstruction) sizes and topologies which have provided very useful knowledge. This has provided a dual approach in parallel with ultrasound and MRI technology elaborating key phenomena

associated with the etiology of obstructions in the kidney and also ureteral system. It is observed that significant progress has been made in understanding the physiology of microliths behavioural pattern due to urinary flow. The strong compressive wave action proceed its direction towards from abdominal region of the ureter to the area of pelvis which results in urinary reflux. From this quantifying analysis, the observation of microliths size is highly important. The particles that exist in filtration of kidney combine to form as sedimentation when it is not filtered properly. Then if the sedimentation is enhanced, finally tends to the stage of renal failure.<sup>[100, 101]</sup> The precaution procedure for this situation is surgical intervention. To avoid those anisotropic behaviour in the wall of the ureter, clinical visit should be the better solution when there is struggle in the normal urine flow. Some key findings are crystallized below based on numerous studies reviewed herein.

- The flow pattern is disturbed significantly by solid particles e.g. stones (monoliths).
- Experiments disclosed the interrelation between pressure gradient, velocity profile, shear stress, bolus trapping when the urine is passing through ureter with or without stones.
- There is gradual decrease in the pressure values when the bolus reaches the outlet.
- At the time of collision between boluses inside the ureter, the pressure gradient reaches generally attains a peak.
- As soon as the bolus hits the outlet, the pressure gradient becomes negative, and this encourages the backflow of urine. This backflow provides a mechanism for antigen entry into the ureter and contributes to renal failure.

Future studies may explore more detailed mesh refinement in the sliding interface between the monoliths and ureteral walls and also consider deformability of deposits and particle (mass) transfer during propulsion.

#### **ETHICAL STATEMENT:**

- **Funding:** N/A
- **Conflict of Interest:** Authors declare that there is no conflict of interest among the authors.
- **Ethical approval:** N/A
- **Informed consent:** N/A

- **Author contribution:**

P. Deepalakshmi, G. Shankar, E. P. Siva, have made substantial contributions to the conception and design of the study; acquisition, analysis, and interpretation of data. D. Tripathi, O. Anwar Bég, and S. Kuharat have made the drafting of the article or revising it critically for important intellectual content and final approval of the version to be submitted.

- **Data Availability Statement (Required):** N/A

## References

1. Boyarsky, S., Labay. P. C., “Ureteral dimensions and specifications for bioengineering modeling” *Urodynamics*, Academic Press. 1971; 163-165
2. Smith, H.W., Goldring, W., & Chasis, H., “The measurement of the tubular excretory mass, effective blood flow and filtration rate in the normal human kidney” *J. Clin. Invest.* 1938; 17(3): 263-278
3. Kiil, F., “Urinary flow and ureteral peristalsis” *Urodynamics: Upper and Lower Urinary Tract*, W. Lutzeyer, H. Melchior (Eds), New York. 1973
4. Thomas, S. R., “Modelling and simulation of the kidney” *Journal of Biological Physics and chemistry.* 2005;5(2/3):70
5. Hammad, F.T., “Electrical propagation in the renal pelvis, ureter and bladder” *Acta Physiologica.* 2015; 213(2): 371-383
6. Griffiths, D. J., & Rollema J., “Urine flow curves of healthy males: a mathematical model of bladder and urethral function during micturition” *Medical and Biological Engineering.* 1979; 17: 291-300
7. Guyton. A., & Hall, J., “Urine formation by the kidneys: I. glomerular filtration, renal blood flow, and their control” In *Textbook of Medical Physiology*, New York. 2006
8. Lykoudis, P. S., “The ureter as a peristaltic pump” *Urodynamics*, Academic Press, New York. 1971; 199-215
9. Pozrikidis, C., “A study of peristaltic flow” *Journal of Fluid Mechanics*, 1987;180:515-27
10. Lang, R.J., Exintaris, B., Teele, M.E., Harvey, J. & Klemm, M.F., “Electrical basis of peristalsis in the mammalian upper urinary tract” *Clinical and Experimental Pharmacology and Physiology.* 1998; 25(5):310-21
11. Weber, E.J., Chapron, A., Chapron, B.D., Voellinger, J.L., Lidberg, K.A., Yeung, C.K., Wang, Z., Yamaura, Y., Hailey, D.W., Neumann, T., & Shen, D.D., “Development of a

- microphysiological model of human kidney proximal tubule function” *Kidney international*. 2016 ;90(3):627-37
12. Keni, L.G., Kalburgi, S., Hameed, B.Z., Zuber, M., Tamagawa, M. & Shenoy, B.S., “Finite element analysis of urinary bladder wall thickness at different pressure condition” *J. Mech. Med. Biol.* 2019;19(05):1950029
  13. Evan, A.P., “Physiopathology and etiology of stone formation in the kidney and the urinary tract” *Pediatric nephrology*. 2010; 25:831-41
  14. Ohlson, L. A., “Morphological dynamics of ureteral transport. I. Shape and volume of constituent urine fractions” *American Journal of Physiology-Regulatory, Integrative and Comparative Physiology*. 1989 ;256(1): R19-28.
  15. Weinstein, A.M., “A mathematical model of rat collecting duct I. Flow effects on transport and urinary acidification” *American Journal of Physiology-Renal Physiology*. 2002;283(6): F1237-51
  16. Singh, P.P., Kumar, G., & Raghav, S., “Peristaltic Flow of Jeffrey Fluid through a slanted cylinder” *Journal of Algebraic Statistics*. 2022 ;13(2):3689-95
  17. Abd-Alla, A.M., & Abdallah, M., “Effect of heat transfer and rotation on the peristaltic flow of a micropolar fluid in a vertical symmetric channel” *Sohag Journal of Sciences*. 2022 ;7(3):117-22
  18. Gendy, M. E., Bég, O.A., Kadir, A., Islam, M.N., & Tripathi, D., “Computational fluid dynamics simulation and visualization of Newtonian and non-Newtonian transport in a peristaltic micro-pump” *J. Mech. Med. Biol.* 2021;21(08):2150058
  19. Duseyy, M.P., “Numerical analysis of lubrication theory and peristaltic transport in the oesophagus” *The Pennsylvania State University ProQuest Dissertations Publishing*. 1993
  20. Manton, M. J., “Long-wavelength peristaltic pumping at low Reynolds number” *J. Fluid Mech.* 1975;68(3):467-76
  21. Griffiths, D. J., “Flow of urine through the ureter: a collapsible, muscular tube undergoing peristalsis”, *ASME J. Biomechanical Engineering*. 1989:206-211
  22. Carew, E.O., & Pedley, T. J., “An active membrane model for peristaltic pumping: part i—periodic activation waves in an infinite tube” *ASME J. Biomechanical Engineering*. 1997; 66-76.
  23. Jiménez-Lozano, J., Sen, M., & Dunn, P.F., “Particle motion in unsteady two-dimensional peristaltic flow with application to the ureter” *Physical Review E—Statistical, Nonlinear, and Soft Matter Physics*. 2009 ;79(4):041901

24. Jiménez-Lozano, J., & Sen, M., “Particle dispersion in two-dimensional peristaltic flow”, *Physics of Fluids*, 2010 ;22(4)
25. Chrispell, J., & Fauci, L., “Peristaltic pumping of solid particles immersed in a viscoelastic fluid” *Mathematical Modelling of Natural Phenomena*, 2011; 6(5):67-83
26. Jaffrin, M. Y., & Shapiro, A. H., “Peristaltic pumping” *Annu. Rev. Fluid Mech.*, 1971;3(1):13-37
27. Jiménez-Lozano, J., Sen, M., & Corona, E., “Analysis of peristaltic two-phase flow with application to ureteral biomechanics” *Acta mechanica*. 2011 ;219(1):91-109
28. Srivastava, L. M., & Srivastava, V. P., “Peristaltic transport of a two-layered model of physiological fluid” *Journal of Biomechanics*. 1982 ;15(4):257-65
29. Riaz, A. and Sadiq, M.A., “Particle–fluid suspension of a non-Newtonian fluid through a curved passage: an application of urinary tract infections” *Frontiers in Physics*. 2020; 8:109
30. Bhatti, M. M., Zeeshan, A., Asif, M. A., Ellahi, R., & Sait, S. M., “Non-uniform pumping flow model for the couple stress particle-fluid under magnetic effects” *Chem. Eng. Commun.* 2022 ;209(8):1058-69
31. Kinn, A. C., “Progress in urodynamic research on the upper urinary tract: implications for practical urology” *Urological research*. 1996; 24:1-7
32. Barton, C., & Raynor, S., “Peristaltic flow in tubes”, *Bull. Mathematical Biophysics*, 1968;30:663-80
33. Vahidi, B., & Fatourae, N., “A numerical simulation of peristaltic motion in the ureter using fluid structure interactions” *29th Annual International Conference of the IEEE Engineering in Medicine and Biology Society*. 2007: 1168-1171
34. Sokolis, D.P., “Multiaxial mechanical behaviour of the passive ureteral wall: experimental study and mathematical characterisation” *Comput method Biomec*. 2012 ;15(11):1145-56
35. Hosseini, G., Williams, J. J., Avital, E. J., Munjiza, A., Dong, X., & Green, J. S., “Simulation of the upper urinary system” *Critical Reviews in Biomedical Engineering*, 2013;41(3)
36. Vahidi, B., & Fatourae, N., “Mathematical modeling of the ureteral peristaltic flow with fluid structure interaction” *Measurements*. 2007; 5(6)
37. Vahidi, B., Fatourae, N., Imanparast, A., & Moghadam, A. N., “A mathematical simulation of the ureter: effects of the model parameters on ureteral pressure/flow relations” *ASME J. Biomechanical Engineering*, 2011; 031004
38. Kim, K.W., Choi, Y.H., Lee, S.B., Baba, Y., Kim, H. H., & Suh, S. H., “Analysis of urine flow in three different ureter models”, *Comput. Math. Methods Med*. 2017(1), p.5172641

39. Vahidi, B., & Fatourae, N., "A biomechanical simulation of ureteral flow during peristalsis using intraluminal morphometric data" *J. Theor. Biol.* 2012; 298:42-50
40. Takaddus, A.T., Gautam, P., & Chandy, A.J., "A fluid-structure interaction (FSI)-based numerical investigation of peristalsis in an obstructed human ureter" *Int. j. numer. method. biomed. eng.* 2018 ;34(9): e3104
41. Najafi, Z., Gautam, P., Schwartz, B. F., Chandy, A. J., & Mahajan, A.M., "Three-dimensional numerical simulations of peristaltic contractions in obstructed ureter flows" *J. Biomech. Eng.* 2016 ;138(10):101002
42. Gómez-Blanco, J. C., Martínez-Reina, F. J., Cruz, D., Pagador, J. B., Sánchez-Margallo, F.M., & Soria, F., "Fluid structural analysis of urine flow in a stented ureter" *Comput. Math. Methods Med.* 2016;2016(1):5710798
43. Liu, Y., Li, M., Qiang, L., Sun, X., Liu, S. & Lu, T. J., "Critical size of kidney stone through ureter: A mechanical analysis" *Journal of the Mechanical Behavior of Biomedical Materials.* 2022; 135:105432
44. Morales, P. A., Crowder, C. H., Fishman, A. P., & Maxwell, M. H., "The response of the ureter and pelvis to changing urine flows" *The Journal of urology.* 1952 ;67(4):484-91
45. Najafi, Z., Schwartz, B. F., Chandy, A. J., & Mahajan, A.M., "A two-dimensional numerical study of peristaltic contractions in obstructed ureter flows" *Computer Methods in Biomechanics and Biomedical Engineering.* 2018 ;21(1):22-32
46. Patankar, S.V., "Numerical Heat Transfer and Fluid Flow", CRC Press, 2018
47. Takaddus, A.T., & Chandy, A. J., "A three-dimensional (3D) two-way coupled fluid-structure interaction (FSI) study of peristaltic flow in obstructed ureters" *Int. j. numer. method. biomed. eng.* 2018 ;34(10): e3122.
48. Morita, T., Wada, I., Saeki, H., Tsuchida, S., & Weiss, R. M., "Ureteral urine transport: changes in bolus volume, peristaltic frequency, intraluminal pressure and volume of flow resulting from autonomic drugs" *The Journal of urology,* 1987 ;137(1):132-5
49. Ishii, T., Naya, Y., Yamanishi, T., & Igarashi, T., "Urine flow dynamics through the urethra in patients with bladder outlet obstruction" *J. Mech. Med. Biol.* 2014 ;14(04):1450052
50. Tanveer, A. & Mahmood, S., "Electroosmosis peristaltic flow with the domination of internal and activation energies for non-Newtonian fluid" *Waves in Random and Complex Media.* 2022:1-13
51. Takaddus, A.T., & Chandy, A. J., "A two way fully coupled fluid structure simulation of human ureter peristalsis" *Computer Methods in Biomechanics and Biomedical Engineering.* 2018: 21(14), 750-759

52. Bevan, T., Carriveau, R., Goneau, L., Cadieux, P., & Razvi, H., "Numerical simulation of peristaltic urine flow in a stented ureter" *American Journal of Biomedical Science*. 2012;4(3):233-48
53. Keni, L. G., Hayoz, M. J., Khader, S. M. A., Hegde, P., Prakashini, K., Tamagawa, M., Shenoy, B.S., Hameed, B. Z., & Zuber, M., "Computational flow analysis of a single peristaltic wave propagation in the ureter" *Computer Methods and Programs in Biomedicine*. 2021; 210:106378
54. Deepalakshmi, P., Darvesh, A., Garalleh, H. A., Sánchez-Chero, M., Shankar, G., Siva, E. P., "Integrate mathematical modeling for heat dynamics in two-phase casson fluid flow through renal tubes with variable wall properties" *Ain Shams Engineering Journal*. 2025;16(1):103183
55. Burns, J. C., Parkes, T., "Peristaltic motion" *J. Fluid Mech*. 1967; 29(4):731-43
56. Khabazi, N. P., & Sadeghy, K., "Peristaltic transport of solid particles suspended in a viscoplastic fluid: a numerical study" *J. Nonnewton. Fluid Mech*. 2016; 236:1-7
57. Shapiro, A. H., & Jaffrin, M. Y., "Weinberg SL. Peristaltic pumping with long wavelengths at low Reynolds number" *J. Fluid Mech*. 1969 ;37(4):799-825
58. Yin, F. C., Fung, Y. C., "Mechanical properties of isolated mammalian ureteral segments" *American Journal of Physiology-Legacy Content*. 1971 ;221(5):1484-93
59. Najafi, Z., "Development of new treatment modalities for kidney/ureter stones" The University of Akron. 2015
60. Hering, F., Briellmann, T., Lüönd, G., Guggenheim, H., Seiler, H., & Rutishauser, G., "Stone formation in human kidney" *Urological research*. 1987; 15:67-73
61. Basavaraj, D. R., Biyani, C. S., Browning, A. J., & Cartledge, J. J., "The role of urinary kidney stone inhibitors and promoters in the pathogenesis of calcium containing renal stones" *EAU-EBU update series*. 2007 ;5(3):126-36
62. McCaig, F., Tomlinson, J., & Harber, M., "Acquired Urinary Tract Obstruction/Obstructive Uropathy" *Primer on Nephrology*. 2022: 993-1017
63. Wilson, J., Farrow, E., & Holden, C., "Urinary tract obstruction" *InnovAiT*. 2022;15(5):265-71
64. Bagley, D. H., Hubosky, S. G., "Difficult Access to the Ureter" *Advanced Ureteroscopy: A Practitioner's Guide to Treating Difficult Problems*. 2022:1-3
65. Coe, F.L., Evan, A., Worcester, E., "Kidney stone disease" *The Journal of clinical investigation*. 2005 ;115(10):2598-608

66. Boone, A. W., Smith, A. G., “The elastic properties of normal ureter” *The Journal of Urology*. 1955 ;73(3):481-6
67. Saeki, H., Morita, T., Nishimoto, T., Kondo, S., Tsuchida, S., “Changes in the ureteral peristaltic rate and the bolus volume in gradual and rapid urinary flow increase” *The Tohoku journal of experimental medicine*. 1985;146(3):273-5
68. Malin, J. M., Boyarsky, S., Labay, P., Gerber, C., “In vitro isometric studies of ureteral smooth muscle” *The Journal of Urology*. 1968 ;99(4):396-8
69. Keni, L. G., Hayoz, M. J., Shenoy, S., Hegde, P., Prakashini, K., Tamagawa, M., Khader, S. M., & Zuber, M., “Ureterodynamic analysis of multiple peristaltic waves on variable diameter ureter” *Engineered Science*. 2022; 17:256-65
70. Griffiths, D. J., & Notschaele, C., “The mechanics of urine transport in the upper urinary tract: 1. The dynamics of the isolated bolus” *Neurourology and Urodynamics*. 1983;2(2):155-66
71. Bevan, T., Carriveau, R., Goneau, L., Cadieux, P., & Razvi, H., “Numerical simulation of peristaltic urine flow in a stented ureter” *American Journal of Biomedical Science*. 2012;4(3):233-48
72. Kumar, B. R., Naidu, K. B., “A numerical study of peristaltic flows” *Computers & fluids*. 1995;24(2):161-76
73. Constantinou, C. E., & Hrynczuk, J. R., “Urodynamics of the upper urinary tract” *Investigative urology*. 1976;14(3):233-40
74. Notley R. G., “The Musculature of The Human Ureter 1” *British Journal of Urology*. 1970;42(6):724-7
75. Damaser, M. S., Lehman, S. L., “The effect of urinary bladder shape on its mechanics during filling” *Journal of biomechanics*. 1995 ;28(6):725-32
76. Keni, L. G., Shenoy, S., Hegde, P., Prakashini, K., Tamagawa, M., Khader, S. M., Hameed B. Z., & Zuber, M., “Investigating the effect of a single peristalsis wave on unobstructed ureter using a computational technique” *Engineered Science*. 2022 ;20(3):330-40
77. Riaz, A., Sadiq, M. A., “Particle–fluid suspension of a non-Newtonian fluid through a curved passage: an application of urinary tract infections” *Frontiers in Physics*. 2020; 8:109
78. Vahidi, B., & Fatouraei, N., “Computational modeling of ureteral peristaltic transport using fluid structure interaction” *Summer Bioengineering Conference 2007*: 47985, 455-456

79. Rassoli, A., Shafigh, M., Seddighi, A., Seddighi, A., Daneshparvar, H., Fatouraee, N., “Biaxial mechanical properties of human ureter under tension” *Urology journal*. 2014;11(3):1678-86
80. Rudyk, R., Malinowski, M., Mackiewicz, A., Bedzinski, R., Noszczyk-Nowak, A., Skonieczna, J., Madej, J. P., “Numerical analysis of deformation and flow in the proximal area of the urethra” *International Journal of Applied Mechanics and Engineering*. 2020;25(2):130-41
81. Hosseini, G., Ji, C., Xu, D., Rezaienia, M.A., Avital, E., Munjiza, A., Williams, J.J.R., & Green, J. S. A., “A computational model of ureteral peristalsis and an investigation into ureteral reflux” *Biomed Eng Lett*. 2017, 8(1):117-125
82. Hanley, H. G., “Transient Stasis and Reflux in The Lower Ureter 1” *British journal of urology*. 1962 ;34(3):283-5
83. Shankar, G., Tripathi, D., Deepalakshmi, P., Anwar Bég, O., Kuharat, S. and Siva, E.P., “A review on blood flow simulation in stenotically diseased arteries”, 2024.
84. Eytan, O., Jaffa, A. J., & Elad, D., “Peristaltic flow in a tapered channel: application to embryo transport within the uterine cavity” *Medical engineering & physics*. 2001;23(7):475-84
85. Xiao, Q., Damodaran, M., “A numerical investigation of peristaltic waves in circular tubes” *Int. J. Comput. Fluid Dyn.*, 2002 ;16(3):201-16
86. Shankar, G., Siva, E.P., Tripathi, D., & Beg, O.A., “Thermal analysis in unsteady oscillatory Darcy blood flow through stenosed artery” *International Journal of Thermofluids*. 2024; 24:100864
87. Misra, J. C., Pandey, S. K., “Peristaltic flow of a multilayered power-law fluid through a cylindrical tube” *Int. J. Eng. Sci.* 2001;39(4):387-402
88. Shashi, K. K., Lee, T., Kurugol, S., Garg, H., Ghelani, S. J., Nelson, C. P., & Chow, J. S., “Normative values for ureteral diameter in children” *Pediatric Radiology*. 2022;52(8):1492-9
89. Rose, J. G., Gillenwater, J. Y., “Pathophysiology of ureteral obstruction” *American Journal of Physiology-Legacy Content*. 1973;225(4):830-7
90. Eisner, B. H., Reese, A., Sheth, S., & Stoller, M. L., “Ureteral stone location at emergency room presentation with colic” *The Journal of urology*. 2009;182(1):165-8
91. Lam, H. S., Lingeman, J. E., Russo, R., & Chua, G. T., “Stone surface area determination techniques: a unifying concept of staghorn stone burden assessment” *The Journal of urology*. 1992;148(3):1026-9

92. Prstojevic, J. K., Junuzovic, D., Hasanbegovic, M., Lepara, Z., & Selimovic, M., "Characteristics of calculi in the urinary tract" *Materia socio-medica*. 2014;26(5):297
93. Ho, Y.S., Lau, C.F., Lee, K., Tan, J.Y., Lee, J., Yung, S. & Chang, R.C.C., "Impact of unilateral ureteral obstruction on cognition and neurodegeneration" *Brain Research Bulletin*. 2021; 169:112-27
94. Kim, H.H., Choi, Y.H., Lee, S.B., Baba, Y., Kim, K.W., & Suh, S.H., "Numerical analysis of the urine flow in a stented ureter with no peristalsis" *Bio-medical materials and engineering*. 2015;26(s1): S215-23
95. Haas, C.R., Shah, O., & Hyams, E.S., "Temporal trends and practice patterns for inpatient management of malignant extrinsic ureteral obstruction in the United States" *Journal of Endourology*. 2020;34(8):828-35
96. Izumi, K., Shima, T., Shigehara, K., Sawada, K., Naito, R., Kato, Y., Ofude, M., Kano, H., Iwamoto, H., Yaegashi, H., & Nakashima, K., "A novel risk classification score for malignant ureteral obstruction: a multicenter prospective validation study" *Scientific Reports*, 2021;11(1):4455
97. Haifler, M., Kleinmann, N., & Weiss, D., "Tandem ureteral stents drainage lowers renal pelvis pressure in malignant ureteral obstruction: Experimental and computational models" *Journal of Biomechanics*. 2021; 117:110237
98. Deepalakshmi, P., Siva, E. P., Tripathi, D., Bég, O. A., & Kuharat, S., "MHD peristaltic two-phase Williamson fluid flow, heat and mass transfer through a ureteral tube with microliths: Electromagnetic therapy simulation" *Numerical Heat Transfer, Part A: Applications*. 2024; 85(20):1-24
99. Zheng, J., Pan, J., Qin, Y., Huang, J., Luo, Y., Gao, X., & Zhou, X., "Role for intravesical prostatic protrusion in lower urinary tract symptom: a fluid structural interaction analysis study" *BMC urology*, 2015;15:1-9
100. Shankar, G. & Siva, E.P., "A Numerical Investigation of Thermal and Mass Exchange of Blood Along Porous Stenosis Arterial Flow with Applied Magnetic Field" *IAENG International Journal of Applied Mathematics*. 2024; 54(3):532-541
101. Barzegari, M., Vahidi, B., Safarinejad, M. R., & Ebad, M., "A computational analysis of the effect of supporting organs on predicted vesical pressure in stress urinary incontinence" *Medical & Biological Engineering & Computing*, 2020;58:1079-89